

AN ANALYTICAL METHOD TO IDENTIFY REINFORCED CONCRETE WALLS PRONE TO OUT-OF-PLANE SHEAR FAILURE

A. NIROOMANDI¹, S. PAMPANIN², R.P. DHAKAL³, M. SOLEYMANI ASHTIANI⁴

¹ PhD, Department of Civil and Natural Resources Engineering, University of Canterbury; Structural Engineer, WSP-Opus. E-mail: Arsalan.niroomandi@wsp.com

² Professor, Department of Structural and Geotechnical Engineering, University of Roma "La Sapienza"; Adjunct Professor, Department of Civil and Natural Resources Engineering, University of Canterbury. E-mail: stefano.pampanin@uniroma1.it; stefano.pampanin@canterbury.ac.nz

³ Professor, Department of Civil and Natural Resources Engineering, University of Canterbury. E-mail: Rajesh.Dhakal@canterbury.ac.nz

⁴ PhD, Supervisor from Industry, Department of Civil and Natural Resources Engineering, University of Canterbury. E-mail: ms.ashtiani81@gmail.com

ABSTRACT: One of the failure modes that got the attention of researchers in the 2011 February New Zealand earthquake was the collapse of a key supporting structural wall of Grand Chancellor Hotel in Christchurch which failed in a brittle manner. However, until now this failure mode has been still a bit of a mystery for the researchers in the field of structural engineering. Moreover, there is no method to identify, assess and design the walls prone to such failure mode. Following the recent break through regarding the mechanism of this failure mode based on experimental observations (out-of-plane shear failure), a numerical model that can capture this failure was developed using the FE software DIANA. A comprehensive numerical parametric study was conducted to identify the key parameters contributing to the development of out-of-plane shear failure in reinforced concrete (RC) walls. Based on the earthquake observations, experimental and numerical studies conducted by the authors of this paper, an analytical method to identify walls prone to out-of-plane shear failure that can be used in practice by engineers is proposed. The method is developed based on the key parameters affecting the seismic performance of RC walls prone to out-of-plane shear failure and can be used for both design and assessment purposes.

1. Introduction

The performance of RC structural wall buildings in earthquakes has generally been robust, and complete collapse under even extreme seismic excitation is rare (Priestley et al. 2007). However, following the two earthquakes in 2010 and 2011 in Chile and New Zealand, some peculiar failure modes were observed in RC structural walls that researchers did not expect (Dunning Thornton 2011, Kam et al. 2011, Elwood et al. 2012, Elwood 2013, NIST 2014). One of these failure modes was the collapse of Wall D5-6 from Grand Chancellor Hotel in the 2011 February earthquake in Christchurch, New Zealand (Figure 1). Different explanations were suggested by researchers for the failure mode observed in this wall including a lateral instability failure, a pure product of axial load and a failure derived from bi-directional loading. Kam et al. (2011) and Niroomandi et al. (2018b) showed that the earthquake loading pattern of the February 2011 earthquake (with 6.2 Magnitude) was a skewed loading with a strong directionality towards the out-of-plane of Wall D5-6 suggesting a strong involvement of bi-

directional loading in the failure of the wall (Figure 2). The fact that Wall D5-6 had no apparent damage under September 2010 earthquake with 7.1 Magnitude with a directionality towards the in-plane of the wall supports this hypothesis.

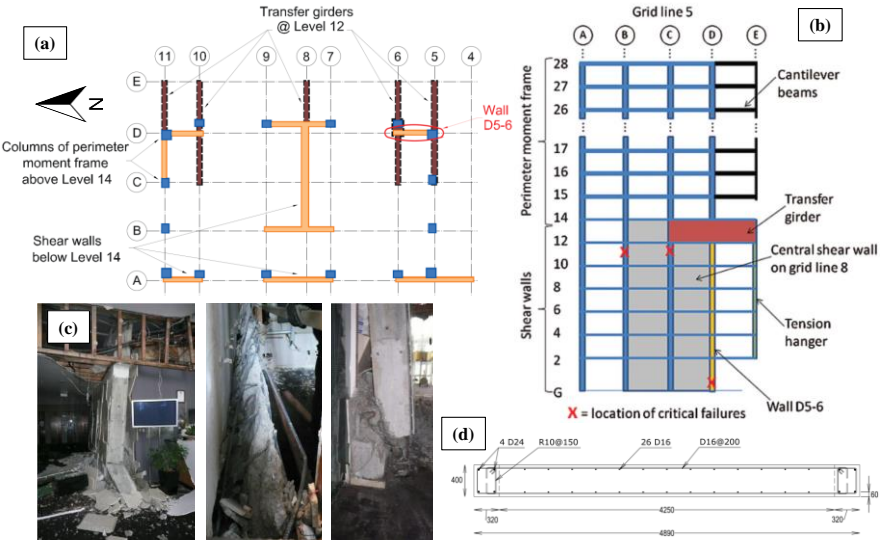


Figure 1 (a & b) Grand Chancellor Hotel structural layout sketch plan and elevation along grid line 5 (Elwood 2013), (c) failure mode of wall D5-6 from GCH building in the 2011 NZ earthquake (Dunning Thornton 2011) and (d) details of the wall D 5-6 (Dunning Thornton 2011)

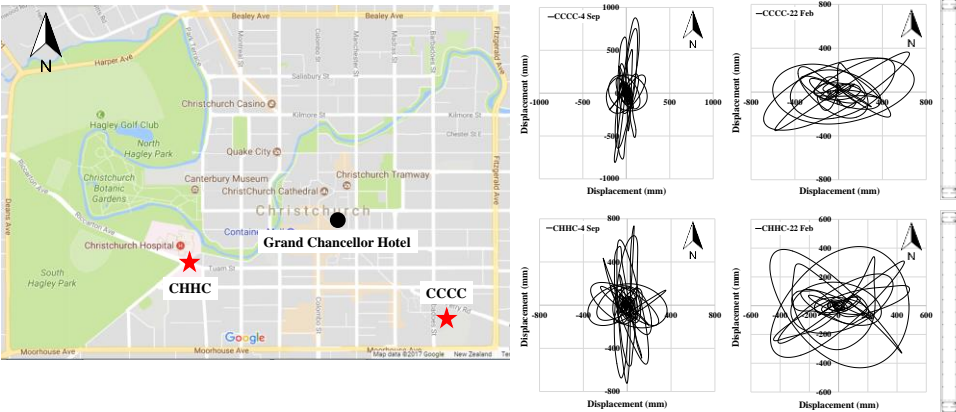


Figure 2 The directionality of ground motions from the 2 September 2010 and 22 February 2011 earthquakes recorded at two stations (CHHC, and CCCC) is illustrated via orbit plots of displacement response which were created by plotting the displacement response of a SDOF element to the N-S component of ground motion versus the displacement response of a SDOF system to the E-W component of ground motion using periods of 2.4 and 2.8 seconds in the N-S and E-W directions, respectively, to represent the fundamental period of the structure in each respective orientation (Niroomandi et al. 2018b)

In this paper, this hypothesis is further investigated numerically and experimentally and the mechanism of the failure mode observed is discussed in more details based on experimental results and a strut and tie model. Finally an analytical method is proposed based on a comprehensive numerical parametric study that can be used by engineers to identify structural walls prone to this failure mode for both design and assessment purposes.

2. Numerical case study on Wall D5-6

Niroomandi et al. (2018b) conducted a numerical study on Wall D5-6 based on FE analysis using DIANA software (DIANA 2015). They found that while no out-of-plane diagonal cracks were observed in the wall under in-plane loading, significant out-of-plane diagonal cracks formed along the entire length of the wall when subjected to a lateral loading pattern similar to February 2011 earthquake. Previously, in an experimental study, Niroomandi et al. (2018a) reported out-of-plane diagonal cracks in slender walls subjected to skew loading. This observation initiated the idea that this type of loading pattern might lead to failure mode such

as the one observed in Wall D5-6. Further numerical investigation was conducted on Wall D5-6 when subjected to lateral loading pattern with different loading angle (Figure 3). The results of this investigation showed that with the increase in the loading angle with respect to the in-plane axis, the possibility of triggering a failure mode similar to the one observed in Wall D5-6 increases. Skew loading with 85° was found to be the worst case scenario in triggering this failure mode (Figure 4). Comparing the loading patterns shown in Figure 3d & Figure 3e reveals that Wall D5-6 was subjected to a type of earthquake loading that could potentially trigger such failure mode. For more information on this numerical study and details of the numerical model including the elements, materials and boundary conditions refer to Niroomandi (2019).

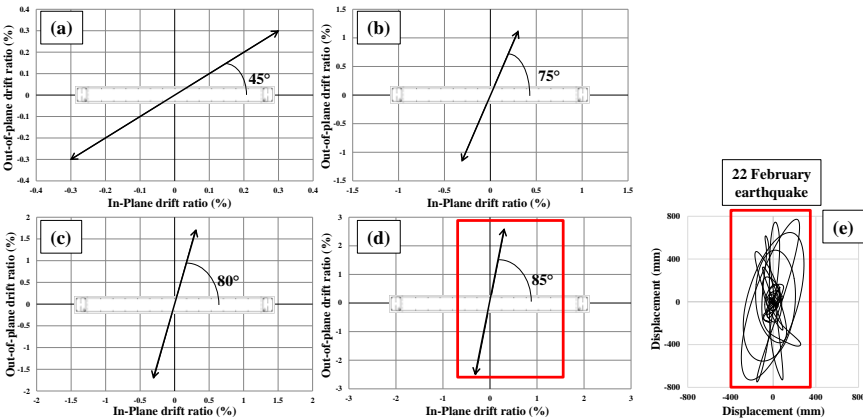


Figure 3 Skewed loading with different loading angles used for the numerical study

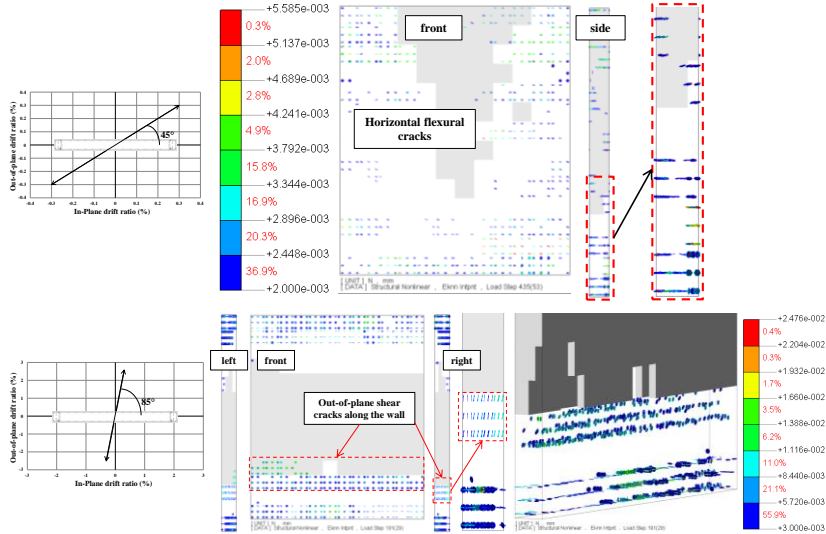


Figure 4 Crack pattern of Wall D5-6 under skew loading with a 45 and 84 degree angles

3. Experimental investigation

In an experimental study conducted by Niroomandi et al. (2018b, 2019), they tested three rectangular slender walls with various section detailing ductility. These walls were tested under a lateral loading pattern similar to the February 2011 earthquake (shown in Figure 3d). Figure 5 shows the failure mode of one of these specimens (SP2-ND). Failure of this specimen involved an out-of-plane diagonal sliding of about 23mm transverse to the wall from its left side, penetrated the full length of the wall and shortened the wall along its height. As can also be seen in Figure 5, all the longitudinal bars along the wall moved down when the wall got shorten along its height after the out-of-plane sliding of the wall. It is worth noting that, no pattern of out-of-plane buckling (global buckling) or longitudinal bar buckling was observed in the wall prior to failure. For more information on specimen SP2-ND and the specimens with higher section detailing ductility (specimens SP3-LD and SP4-D), refer to Niroomandi (2019).

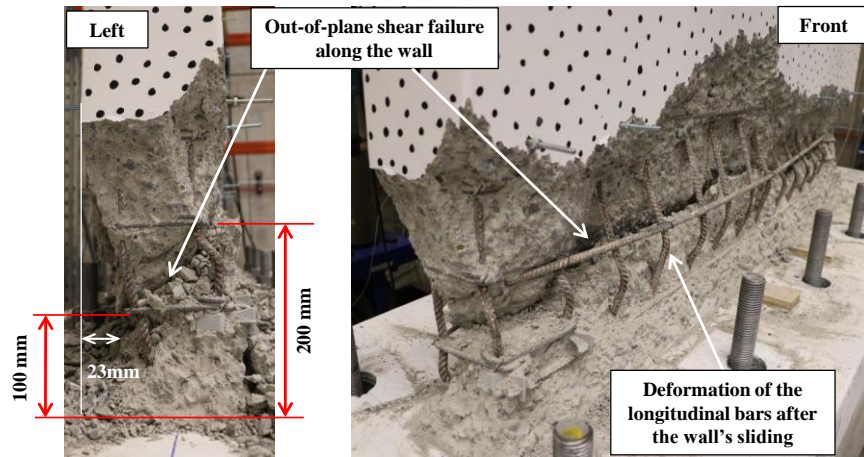


Figure 5 Specimen SP2-ND failure mode after removing the concrete spalling pieces

4. Failure mechanism of specimen SP2-ND

In this section, failure mechanism observed in specimen SP2-ND is scrutinized and described based on the experimental observations, 2D strain profile of the wall and a strut and tie model. Figure 6 shows the 2D strain profile and the strut and tie model of specimen SP2-ND at the peak points of the first cycle of 0.15% in-plane and 1.72% out-of-plane drift ratios. Hatched area of the strain profile shows parts of the wall in compression. It can be seen that failure of the vertical compression strut shown in red in Figure 6, significantly increased the force in the diagonal compression strut. This led to initiation of out-of-plane diagonal compression cracks. The strut and tie model shows the direction of the diagonal cracks which are expected to form under such lateral loading pattern in each side of the wall which matches the experimental observations. It is worth noting that the strain profile plane is also angled which requires 3D strain profile for a more accurate representation. Figure 7 shows the specimen at the peak points of the second cycle of 0.15% in-plane and 1.72% out-of-plane drift ratios. Looking at Figure 7, it can be seen that with the increase in the compressive strain along the wall, forces in the struts and consequently the out-of-plane diagonal compression cracks increased. As shown in Figure 7, during pushing (loading the left-front corner), the entire thickness of the wall is in compression. It can be seen in Figure 7 that 235mm of the left side of the wall from its back is in compression. This shows the penetration of the out-of-plane diagonal compression cracks along the wall in the left side.

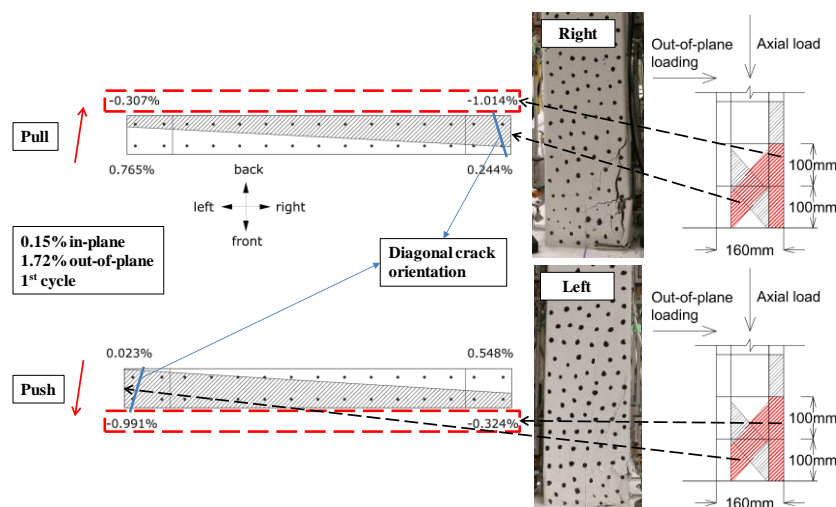


Figure 6 Strut and tie model of specimen SP2-ND at the first cycle of 0.15% in-plane and 1.72% out-of-plane drift ratios

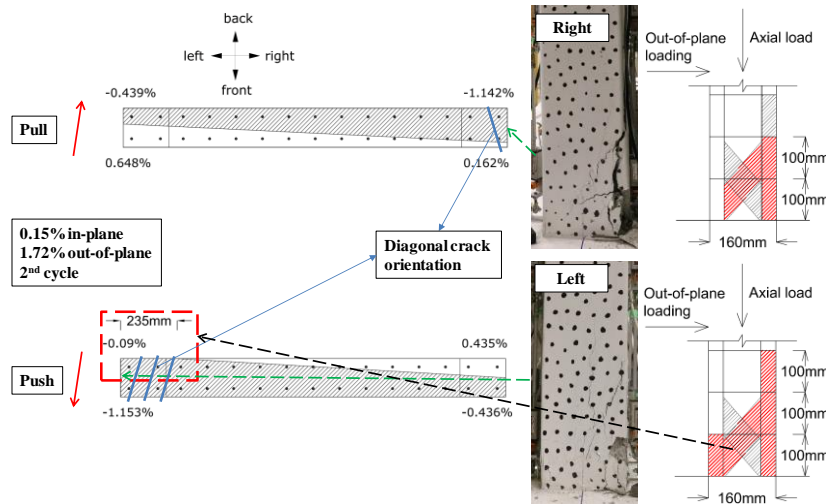


Figure 7 Strut and tie model of specimen SP2-ND at the second cycle of 0.15% in-plane and 1.72% out-of-plane drift ratios

During the peak points of the third cycle of 0.15% in-plane and 1.72% out-of-plane drift ratios (Figure 8), the penetration length of the out-of-plane diagonal compression cracks along the wall from the left side increased to about 600mm (37.5% of the wall's length). During this drift cycle, full diagonal crack was visible along the thickness as the neutral axis depth in the out-of-plane was the full thickness of the wall. Figure 9 shows the 2D strain profile of the wall just before failure during pulling (i.e. half way through the peak, loading the right-back corner). It can be seen that the whole wall was still in compression at that drift level. At this point, the vertical struts along the wall on both sides (front and back) had failed and the diagonal struts were extensively cracked along the wall. Then, the out-of-plane shear applied to the right-back corner led to sliding of the wall in that direction. The name “out-of-plane shear” was chosen for this failure mode to reflect the out-of-plane shear force that led to the final failure of the wall. Figure 9 shows this out-of-plane shear force which is a resultant of the out-of-plane and axial forces along the diagonal crack angle. In the case of SP2-ND since the penetration length of the diagonal cracks on the left side of the wall was considerably larger than the right side, the final failure was towards the back side of the wall (see Figure 8). It is worth mentioning again, the key reason that the out-of-plane diagonal cracks were able to penetrate the entire length of the wall was the bi-directional loading and its effect on the compression area.

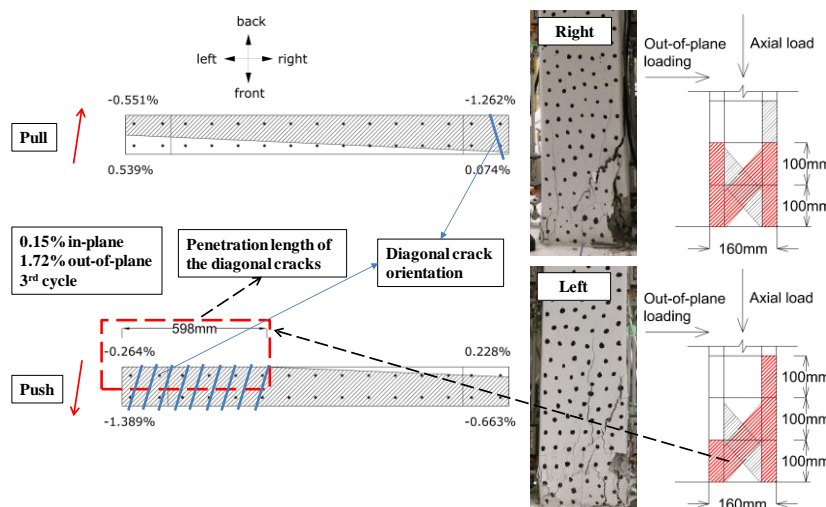


Figure 8 Strut and tie model of specimen SP2-ND at the third cycle of 0.15% in-plane and 1.72% out-of-plane drift ratios

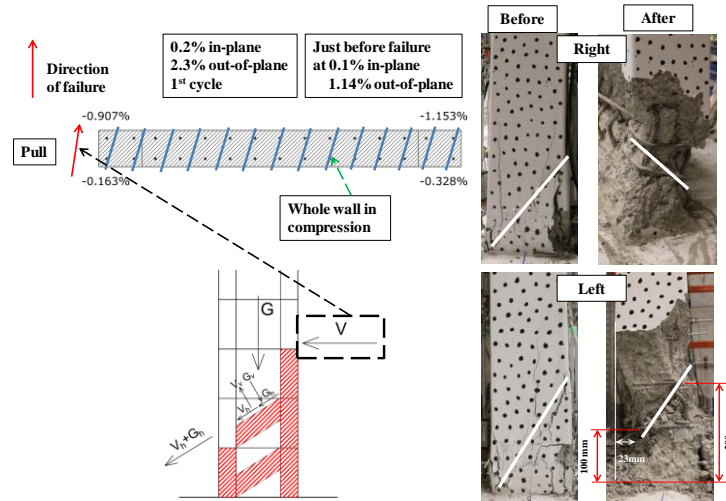


Figure 9 Strut and tie model of specimen SP2-ND just before failure

5. Numerical parametric study on walls prone to out-of-plane shear failure

In Section 2, it was shown that lateral loading pattern can change the failure mode of a rectangular RC wall from a concrete crushing to an out-of-plane shear failure. In this section, while focusing on walls prone to out-of-plane shear failure the effects of other key parameters on the seismic behaviour of rectangular slender walls are investigated.

5.1. Key parameters in developing out-of-plane shear failure

The Axial load ratio, section aspect ratio, section detailing ductility and longitudinal reinforcement ratio were found to be the key parameters in developing out-of-plane shear failure in rectangular slender RC walls. These findings were based on the earthquake observations (February 2011 New Zealand), the numerical study discussed in Section 2 and the experimental results presented in Sections 3 and 4. Effects of each of these parameters on the seismic behaviour of the wall were investigated in a comprehensive numerical study using FE analysis and discussed in Niroomandi (2019). Results of this numerical study is discussed in Sections 5.2-5.5. Table 1 shows the basic characteristics of the walls used for this numerical study. For these investigations, in-plane and out-of-plane shear span ratios, longitudinal and horizontal reinforcement ratio were kept constant. Based on the numerical results discussed in Section 2, these walls were investigated under cyclic skewed loading with 85° angle with respect to the in-plane axis shown in Figure 3d. Nominal ($\mu = 1.25$), limited ($\mu = 1.25 - 3$) and ductile ($\mu \geq 3$) detailing levels in Table 1 are based on NZS3101:2006-A3 (2017).

5.2. Effects of axial load ratio, $P/(A_g f'_c)$

Walls prone to out-of-plane shear failure were investigated under six levels of axial load ratio when subjected to bi-directional loading. Figure 10 shows the geometry and detailing of the walls used for this part of the study. Looking at the von Mises and axial strains contours and the crack patterns of walls with 5% and 20% axial load ratios shown in Figure 11, it can be seen that higher axial load ratio increases the length of the part vulnerable to out-of-plane shear failure (this is discussed in Section 4). Moreover, comparing the von Mises strain pattern of the two walls shown in Figure 11, it can be seen that higher axial load ratio increased the out-of-plane strain. Table 2 shows the failure mode of the walls with different axial load ratios. In terms of failure mode, it was found that flexural failure under low axial load ratio and out-of-plane shear failure under higher axial load ratio were occurred. However, further increase of axial load ratio would change the failure mode to an axial crushing failure.

Table 1 Characteristics of the walls used for the numerical study

| Parameters | Axial load ratio ¹ | Section aspect ratio ² | Section detailing ductility | In-plane shear span ratio ³ | Out-of-plane shear span ratio ⁴ | Longitudinal reinforcement ratio ⁵ | Horizontal reinforcement ratio ⁶ |
|---|-------------------------------|-----------------------------------|-----------------------------|--|--|---|---|
| Axial load ratio ¹ | 5% | 12.2 | Nominal Ductile | 3.45 | 6.69 | 0.45% | 0.503% |
| | 10% | | | | | | |
| | 15% | | | | | | |
| | 20% | | | | | | |
| | 25% | | | | | | |
| 30% | | | | | | | |
| Section aspect ratio ² | 15% | 7.5 | Nominal Ductile | 3.45 | 5.04 | 0.45% | 0.503% |
| | | 9.78 | | | | | |
| | | 12.22 | | | | | |
| | | 16.3 | | | | | |
| Section detailing ductility | 15% | 7.5 | Nominal Ductile | 3.45 | 5.04 | 0.45% | 0.503% |
| | | | Limited Ductile | | | | |
| | | | Ductile | | | | |
| Longitudinal reinforcement ratio ⁵ | 20% | 12.2 | Nominal Ductile | 3.45 | 6.69 | 0.45% | 0.503% |
| | | | | | | 0.75% | |
| | | | | | | 1.5% | |

¹ $P/(A_g f_c')$, using $f_c' = 35MPa$.

² L_w/t

³ H_e/L_w , In-plane shear span of the wall, H_e , is equal to the in-plane effective height of the building

⁴ H_{out}/t , Out-of-plane shear span of the wall, H_{out} , was considered half the length of the first storey height to the slab centre, assuming a double bending deformation shape in the out-of-plane direction

⁵ $\rho_t = (A_{s,BZ} + A_{s,web})/(L_w \times t)$

⁶ $\rho_v = A_{sv}/(s \times t)$

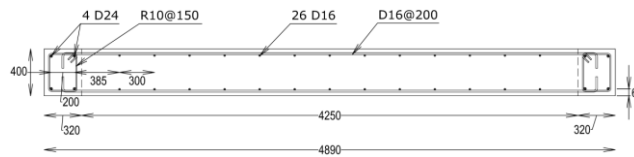


Figure 10 Details of the wall used for the parametric study on axial load ratio

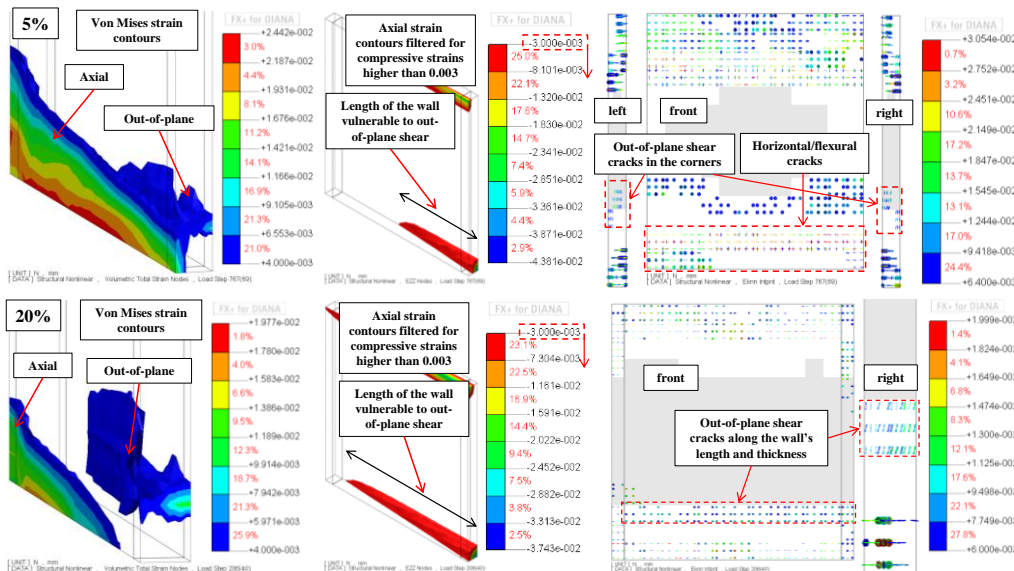


Figure 11 Von Mises and axial strains contours and crack pattern for 5% and 20% axial load ratios

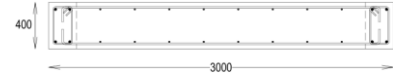
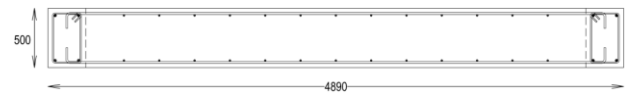
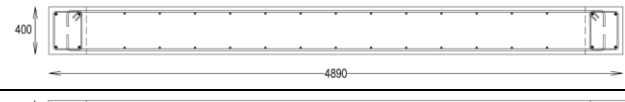
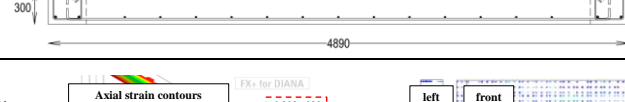
Table 2 Failure mode of the walls with different axial load ratios

| Axial load ratio | Failure mode |
|------------------|-------------------------------------|
| 5% | Flexural |
| 10% | Flexural + concrete crushing |
| 15% | Flexural + concrete crushing |
| 20% | Out-of-plane shear |
| 25% | Axial crushing + out-of-plane shear |
| 30% | Axial crushing |

5.3. Effects of section aspect ratio, (L_w/t)

Table 3 shows the walls used for investigating the effects of section aspect ratio. The investigation was based on the von Mises and axial strain contours and crack pattern of the walls. It can be seen in Figure 12 that lower section aspect ratio increases the area in compression and the out-of-plane diagonal compression cracks.

Table 3 Walls used for the parametric study on section aspect ratio

| Section aspect ratio | Section |
|----------------------|--|
| 7.5 |  |
| 9.78 |  |
| 12.2 |  |
| 16.3 |  |

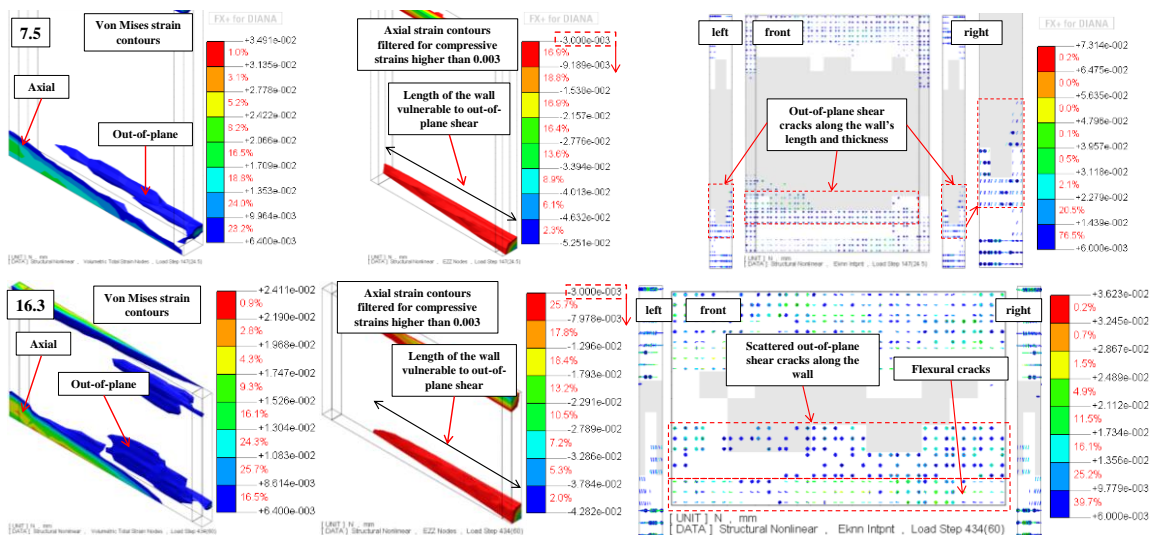


Figure 12 Von Mises and axial strains contours and crack pattern for section aspect ratios of 7.5 and 16.3

5.4. Section detailing ductility

Table 4 shows the details of the walls used for investigating section detailing ductility. Numerical study of this section follows and confirms the experimental findings presented in Niroomandi (2019) that with the increase in the section detailing ductility, the out-of-plane shear failure in the wall may be prevented. Higher section detailing ductility increases the amount of transverse reinforcement in the wall, therefore increases the out-of-plane shear capacity of the wall as well as compressive strength/strain of concrete due to confinement. More transverse reinforcement along the wall was able to prevent the development of out-of-plane diagonal compression cracks in the case of walls designed for limited and ductile levels. Definition of each of these ductility levels were described in Section 5.1. Due to the limitation with the number of pages, numerical results of this part of the study are not presented in this paper. These results can be found in Niroomandi (2019).

5.5. Longitudinal reinforcement ratio, $\rho_t = (A_{s,BZ} + A_{s,web}) / (L_w \times t)$

Comparing the failure mode observed in Wall D5-6 (Figure 1c) with experimental results of specimen SP2-ND as well as the numerical results conducted by Niroomandi (2019), it can be concluded that although higher longitudinal reinforced ratio might not be able to prevent out-of-plane shear failure, it can prevent the full rupture of longitudinal bars observed in Wall D5-6 as can be seen in Figure 5. Due to the limitation with the number of pages, numerical results of this part of the study are not presented in this paper.

Table 4 walls used for the parametric study on section detailing ductility

| Section ductility | Section |
|-------------------|---------|
| Nominal ductile | |
| Limited ductile | |
| Ductile | |

6. Analytical method for identifying walls prone to out-of-plane shear failure

One of the key objectives of this study is to find a method to identify RC walls prone to out-of-plane shear failure. In Section 5, the effects of key parameters on the seismic performance of RC walls prone to out-of-plane shear failure were discussed. Based on these numerical results, it was found that the two important parameters causing vulnerability in walls against out-of-plane shear failure are section aspect ratio and axial load ratio. Therefore, a matrix of walls with a combination of these two parameters is formed. A skewed lateral loading pattern with an 85° angle with respect to the in-plane axis of the wall (Figure 3d), that found to be the worst case loading pattern in terms of triggering out-of-plane shear failure (see Section 2) was used for these analyses. Some of the parameters of the walls used for the matrix were shown in Table 5.

Table 5 Characteristics of the walls used for the parametric study matrix

| Parameters | Section aspect ratio, L_w/t | | | | |
|--|-------------------------------|------|------|------|------|
| | 7.5 | 9.8 | 12.2 | 14 | 16.3 |
| Length, L_w (mm) | 3000 | | | | |
| Thickness, t (mm) | 400 | 500 | 400 | 350 | 300 |
| Out-of-plane shear span [*] , H_{out} (mm) | 2015 | 2520 | 2015 | 1763 | 1512 |
| Out-of-plane shear span ratio, H_{out}/t | 5.04 | | | | |
| In-plane shear span ratio, H_e/L_w | 3.45 | | | | |
| Section detailing ductility | Nominal Ductility | | | | |
| Axial load ratio, $P/(A_g f'_c)$ (%) | 10%, 15%, 20% and 25% | | | | |
| Longitudinal reinforcement ratio (%) $\rho_t = (A_{s,BZ} + A_{s,web}) / (L_w \times t)$ | 0.45 | | | | |
| Horizontal reinforcement ratio (%) $\rho_v = A_w / (s \times t)$ | 0.5 | | | | |
| Compressive strength of concrete (MPa) | 35 | | | | |
| Yield strength of reinforcement (MPa) | 300 | | | | |

* Out-of-plane shear span is half the first floor height

Based on the numerical results of this matrix (Refer to Niroomandi 2019), failure modes captured for walls of different section aspect ratios and axial load ratios were categorized in three groups of flexural, out-of-plane shear and axial crushing failure modes as plotted in Figure 13. Based on these three categories of failure modes, an upper and lower bound limit

curves were developed for the possibility of out-of-plane shear failure in rectangular RC walls (Figure 13). Figure 14 shows the equations of the two curves shown in Figure 13. These curves can be used for engineering purposes when designing/assessing RC walls against out-of-plane shear failure. To use the method shown in Figure 14, engineers only need to have the wall's section aspect ratio and axial load ratio to find whether the wall is prone to out-of-plane shear failure or not. For the lower bound limit shown in Figure 14, the proposed method does not specify the type of flexural failure such as concrete crushing, bar buckling, lateral instability and etc. Other methods should be used to capture these types of failure in the wall. The method shown in Figure 14 was developed only for walls with nominal section detailing ductility. Based on the experimental and numerical results of this study (Refer to Niroomandi 2019 for further details), it is not likely for limited or ductile walls (according to NZS3101:2006-A3 2017) to fail in out-of-plane shear. Although the graph shown in Figure 14 was developed for walls with low longitudinal reinforcement ratio, as was pointed out in Section 5.5, it is likely that walls with higher longitudinal reinforcement ratio experience out-of-plane shear failure as well.

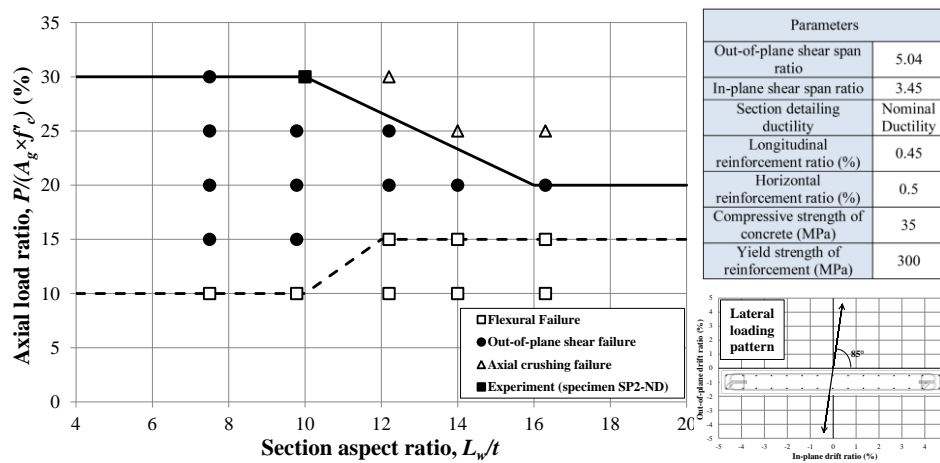


Figure 13 Upper and lower bounds of out-of-plane shear failure in rectangular slender RC walls

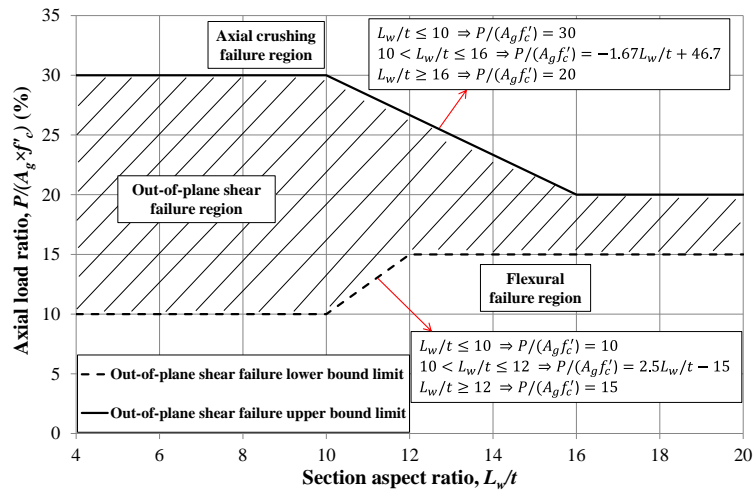


Figure 14 Equations of the upper and lower bound curves of out-of-plane shear failure in rectangular slender RC walls

7. Conclusions

In one of the very first steps towards understanding the effects of bi-directional loading on the seismic behaviour of rectangular slender RC walls and more specifically walls prone to out-of-plane shear failure, a series of experimental and numerical investigations were conducted. The experimental and numerical results as well as earthquake observations indicate the contribution of bi-directional loading in the development of out-of-plane shear failure. Other parameters such as high axial load ratio, low section aspect ratio and low section detailing

ductility were also found to be influential in triggering out-of-plane shear failure. An analytical method was proposed based on a comprehensive numerical parametric study and experimental results that can identify walls prone to out-of-plane shear failure. This method can be used by structural engineers to assess or design RC walls against this failure mode.

8. Acknowledgments

The specimens were tested at the University of Canterbury, Christchurch, New Zealand and Alan Thirlwell (technician of the Structural Engineering Laboratory) contribution was essential for the management of the test setup and for the testing. The financial support of this research, provided by the SAFER Concrete Research Project, funded by the Natural Hazards Research Platform (NHRP), and by the Wall Projects, managed by the UC Quake Centre and funded by the Ministry of Business and Innovation (MBIE) is greatly appreciated. Authors would like to thank Stahlton Engineered Concrete for constructing the specimens and supporting the study.

9. References

- DIANA (2015). DIANA Manual Release 9.6, TNO DIANA BV. Delft, the Netherlands.
- Dunning Thornton (2011). Report on the structural performance of the Hotel Grand Chancellor in the earthquake on 22 February 2011. A report to the Department of Building and Housing (DBH), Dunning Thornton Consultants Ltd., Wellington, New Zealand.
- Elwood, K., S. Pampanin and W. Y. Kam (2012). 22 February 2011 Christchurch earthquake and implications for the design of concrete structures. The International Symposium on Engineering Lessons Learned from the 2011 Great East Japan Earthquake, Tokyo, Japan.
- Elwood, K. J. (2013). "Performance of concrete buildings in the 22 February 2011 Christchurch earthquake and implications for Canadian codes." *Canadian Journal of Civil Engineering* **40**(3): 759-776.
- Kam, W. Y., S. Pampanin and K. J. Elwood (2011). "Seismic performance of reinforced concrete buildings in the 22 February Christchurch (Lyttelton) earthquake." *Bulletin of the New Zealand Society for Earthquake Engineering* **44**(4): 239-278.
- Niroomandi, A. (2019). Seismic Behaviour of Rectangular Reinforced Concrete Walls under Bi-Directional Loading. PhD, University of Canterbury.
- Niroomandi, A., S. Pampanin, R. P. Dhakal and M. Soleymani Ashtiani (2018a). Experimental study on slender rectangular RC walls under bi-directional loading. Eleventh U.S. National Conference on Earthquake Engineering, Los Angeles, California.
- Niroomandi, A., S. Pampanin, R. P. Dhakal, M. Soleymani Ashtiani and C. De La Torre (2018b). Rectangular RC walls under bi-directional loading: recent experimental and numerical findings. The concrete NZ conference, Hamilton, New Zealand.
- NIST (2014). Recommendations for Seismic Design of Reinforced Concrete Wall Buildings Based on Studies of the 2010 Maule, Chile Earthquake.
- NZS3101:2006-A3 (2017). Code of Practice for the Design of Concrete Structures, Standards Association of New Zealand.
- Priestley, M. J. N., M. C. Calvi and M. J. Kowalsky (2007). Displacement-Based Seismic Design of Structures. IUSS Press, Pavia, Italy.